Since January 2020 Elsevier has created a COVID-19 resource centre with free information in English and Mandarin on the novel coronavirus COVID-19. The COVID-19 resource centre is hosted on Elsevier Connect, the company's public news and information website.

Vaccine 30 (2012) 3653–3665

Contents lists available at SciVerse ScienceDirect

Vaccine

journal homepage: www.elsevier.com/locate/vaccine

A virus-like particle vaccine platform elicits heightened and hastened local lung mucosal antibody production after a single dose

Laura E. Richert[a,1], Amy E. Servid[b,1], Ann L. Harmsen[a], Agnieszka Rynda-Apple[a], Soo Han[a], James A. Wiley[a], Trevor Douglas[b,*], Allen G. Harmsen[a,**]

[a] Department of Immunology and Infectious Diseases, Montana State University, Bozeman, MT 59718, United States
[b] Department of Chemistry and Biochemistry, Montana State University, Bozeman, MT 59718, United States

ARTICLE INFO

Article history:
Received 14 October 2011
Received in revised form 17 February 2012
Accepted 16 March 2012
Available online 28 March 2012

Keywords:
Virus-like particle
Nanoparticle
Influenza virus
Mucosal vaccine
Ovalbumin
Tissue-specific Immunity

ABSTRACT

We show that a model antigen, ovalbumin (OVA), can be chemically conjugated to the exterior of a small heat shock protein (sHsp) cage that has structural similarities to virus-like particles (VLPs). OVA–sHsp conjugation efficiency was dependent upon the stoichiometry and the length of the small molecule linker utilized, and the attachment position on the sHsp cage. When conjugated OVA–sHsp was delivered intranasally to naïve mice, the resulting immune response to OVA was accelerated and intensified, and OVA-specific IgG1 responses were apparent within 5 days after a single immunizing dose, illustrating its utility for vaccine development. If animals were pretreated with a disparate VLP, P22 (a non-replicative bacteriophage capsid), before OVA–sHsp conjugate immunization, OVA-specific IgG1 responses were apparent already by 4 days after a single immunizing dose of conjugate in OVA-naïve mice. Additionally, the mice pretreated with P22 produced high titer mucosal IgA, and isotype-switched OVA-specific serum IgG. Similarly, sHsp pretreatment enhanced the accumulation of lung germinal center B cells, T follicular helper cells, and increased polymeric Ig receptor expression, priming the lungs for subsequent IgG and IgA responses to influenza virus challenge. Thus, sHsp nanoparticles elicited quick and intense antibody responses and these accelerated responses could similarly be induced to antigen chemically conjugated to the sHsp. Pretreatment of mice with P22 further accelerated the onset of the antibody response to OVA–sHsp, demonstrating the utility of conjugating antigens to VLPs for pre-, or possibly post-exposure prophylaxis of lung, all without the need for adjuvant.

1. Introduction

Respiratory infections are one of the most prominent afflictions in individuals of all ages and immune statuses, signifying a significant global health concern. Unfortunately, we are currently unable to provide vaccines against many clinically relevant lower respiratory tract pathogens, nor are we able to fully predict the identity of future outbreaks. This global vulnerability has been clearly illustrated by several epidemics in recent memory, including the newly emerged coronavirus, SARS-CoV outbreak of 2002, various influenza strain reassortments (H5N1 "bird flu" and H1N1pandemic), and bioterrorism events involving pathogen aerosolization. Thus, there is an urgent and crucial need for the development of broad-spectrum, rapidly acting vaccination strategies.

Unlike most other mucosal sites in the body, which are protected and immunologically shaped by their commensal microbial communities, the lung is more or less sterile. Therefore, the lung relies on an intricate network of sentinel dendritic cells, antimicrobial secretions, and resident macrophages for defense. Importantly, immune responses in the lung must be tightly regulated to promote immunity, while avoiding tissue damage associated with either the pathogen or the host response. As such, pulmonary immune responses are quite unique, and as suggested by others, the individual history of specific pathogen exposures to the lungs may contribute to shaping the appropriate ensuing immune responses to subsequent challenges [1–4]. Here (and elsewhere [5]), we further demonstrate that virus-like particles (VLPs), which are unrelated to the antigen of subsequent challenge, can similarly impact the lung microenvironment, without the associated pathology, thereby shaping future immune responses. Many groups have previously suggested that the lung may provide an important route of delivery for mucosal vaccination [6–8]. However, the potential

* Corresponding author at: P.O. Box 173400, Bozeman, MT 59717, United States. Tel.: +1 406 994 6566; fax: +1 406 994 5407.
** Corresponding author at: P.O. Box 173610, Bozeman, MT 59717, United States. Tel.: +1 406 994 7626; fax: +1 406 994 4303.
E-mail addresses: tdouglas@chemistry.montana.edu (T. Douglas), aharmsen@montana.edu (A.G. Harmsen).
[1] These authors contributed equally to the work described.

0264-410X/$ – see front matter © 2012 Elsevier Ltd. All rights reserved.
doi:10.1016/j.vaccine.2012.03.035

for utilizing localized mucosal vaccination strategies in the lower respiratory tract have historically been overlooked, and approaches which elicit tissue-specific immune responses are just beginning to be developed. An FDA-approved tribute to the realization of this strategy is the highly effective Flumist vaccine, which is delivered intranasally, and provides better comprehensive local immunity than injectable versions [9–11].

Additionally, the application of nanomaterials to biomedicine is one of the most exciting and potentially revolutionary applications of nanotechnology. Here, we describe a mechanism by which we can enhance primary local immune responses to antigens without the necessity of specific antigen priming. We achieved this result by intranasally delivering empty virus-like particles (VLPs), which act to modulate the lung microenvironment, and harness and focus immune responses. Recent exploration in the utilization of nanoparticles [12–14], virus-like particles [15–21], and viruses which have no mammalian cell tropism, has shown that these platforms are naturally immunostimulatory, and likely utilize evolutionarily conserved cell surface receptors, thereby safely engaging immune signaling pathways without replicating [22–26]. Furthermore, many of these strategies are currently on the market or undergoing clinical trials, and have already had broad global impact in safely preventing disease [21,27–29]. Importantly, virus-like particles can be produced in large quantities, provide a stable product, often are amenable to lyophilization or freeze-drying, and are fiscally economical. These features are especially important for less industrialized nations.

In the following studies we utilize two empty, non-pathogenic virus-like particles – a small heat shock protein cage nanoparticle (sHsp) and the P22 phage-derived virus-like particle (P22) as immunomodulatory antigens in both a non-specific pre-priming scenario, and as a platform for the delivery of specific antigen to the lung. The small heat shock protein 16.5 (sHsp) from *Methanocaldococcus jannaschii* (a hyperthermophilic archaeon) is comprised of 24 repeating subunits [30,31]. These subunits self-assemble to produce an empty cage-like structure, comparable to that of a virus capsid by virtue of the high symmetry and quaternary structure [5,32–34]. We have previously shown that sHsp can be genetically engineered to incorporate cysteine residues, thereby providing attachment sites for bioconjugation [33,35,36], which we exploit here for the display of a foreign protein, similarly to described strategies [37,38]. P22 is a bacteriophage capsid which infects *Salmonella typhimurium* (when intact tail fibers are present) [39,40]. The P22 used here is devoid of both genetic material and tail fibers, and is therefore composed of only the non-infectious empty viral capsid. We would like to note here that previously we have referred to the sHsp nanoparticles as "protein cage nanoparticles" or PCN [5]. However, we now find it to be more descriptive to classify both the sHsp and P22 as virus-like particles, given their structural architecture and immunological parallels to other particles described in the literature. Importantly, neither sHsp nor P22 target known mammalian pattern-recognition receptors, nor do they infect mammalian cells. And while the immunomodulatory potential in exploiting non-pathogenic viruses is still in its infancy, others have begun to describe similar successful strategies [24–26].

P22 and sHsp are herein used as immunomodulatory agents alone in a lung priming strategy to achieve heightened heterologous immunity to distinct antigens, such as OVA and influenza virus; or, in the case of sHsp, as a vaccine delivery platform for a model antigen, OVA, which we have conjugated (in its entirety) to the exterior surface of the sHsp cage. This immunization strategy is advantageous because it accelerates and intensifies the primary immune response, after only a single dose. We further show that conjugating a model antigen (OVA) to sHsp elicits an immune response to OVA which mirrors the response to the sHsp itself. sHsp conjugation also acts to adjuvant OVA, and the local delivery of sHsp and antigen complexes induce potent local IgA secretion in sHsp pretreated mice. Therefore, we show that VLPs (sHsp and P22) can be used as both immunomodulatory agents by pretreating the lung and/or as a carrier of antigens, allowing local immunization of the lower respiratory tract against a pathogen of interest, with a single dose. This platform could be useful for both pre- and post-exposure prophylaxis.

2. Materials and methods

2.1. Production of small heat-shock protein cage nanoparticle (sHsp)

The small heat-shock protein (sHsp 16.5) was initially purified as described previously [33]. In a slight modification of the previously described protocol, the supernatants from 2 L of cell culture were combined and concentrated to 10 mL with a 100k MWCO amicon filter (Millipore, Billerica, MA) prior to size exclusion chromatography on a Superose 6 column (GE Healthcare, Piscataway, NJ) so that purification of large amounts of sHsp could be accomplished efficiently. In order to remove residual protein contaminants, additional steps were added to the previous protocol. The fractions containing sHsp from size exclusion chromatography were re-concentrated to 10 mL and purified by anion exchange on a Sepharose Q column (GE Healthcare) using a linear gradient from 300 mM to 800 mM NaCl in 25 mM HEPES Buffer at pH 7.3. Following this, the fractions containing sHsp were dialyzed overnight into 50 mM phosphate, 100 mM NaCl, and 5 mM EDTA, at pH 7.3, concentrated a third time to 10 mL, and re-subjected to size exclusion chromatography using a Superose 6 column (GE Healthcare) with the same buffer. For the S121C sHsp variant protein, tris(2-carboxyethyl)phosphine (Pierce, Rockford, IL) was added to a final concentration of 2 mM during each amicon concentration step prior to the FPLC runs to inhibit disulfide formation between external thiols on sHsp. The sHsp protein concentration was determined *via* UV–visible spectroscopy using an extinction coefficient of A280 = 0.565 $(mg/mL)^{-1}$ as previously documented [33].

2.2. OVA Preparation

Larger aggregates from commercially available ovalbumin (OVA) (Sigma–Aldrich, Saint Louis, MO, A5503) were removed by size exclusion chromatography using a Superose 6 column (GE Healthcare). Fifty millimolar phosphate, 100 mM NaCl, and 5 mM EDTA at pH 7.3 was used as an elution buffer. Protein concentrations were determined by UV–visible spectroscopy using a previously documented extinction coefficient of A280 = 0.789 $(mg/mL)^{-1}$ for OVA [41].

2.3. P22 preparation

The P22 K118C coat and scaffold protein were expressed in *Escherichia coli*, purified, and assembled *in vitro* as described previously [39]. The purified P22 particles were heated for 20 min at 65 °C to remove the scaffold protein, purified on a sephacryl 500 column (Amersham, Piscataway, NJ), and concentrated to 2 mg/mL, and dialyzed extensively into 50 mM phosphate, 100 mM NaCl, and at pH 7.2. The P22 concentration was calculated using an extinction coefficient A280 = 1.4 $(mg/mL)^{-1}$.

2.4. Optimization of OVA–sHsp conjugation

To determine the initial conditions for conjugation, a matrix of linking conditions were tested. All reactions were carried out in 50 mM phosphate, 100 mM NaCL, 5 mM EDTA, pH 7.3. OVA (80 μL, 7.72 mg/mL) was labeled with a 2-fold molar excess of

each SM(PEG)$_n$ linker (SM(PEG)$_2$, SM(PEG)$_6$, or SM(PEG)$_{12}$) using a stock solution of 25 mM linker in DMSO respectively. These samples were incubated at room temperature for 50 min, and un-conjugated linker was immediately removed using Micro Bio-Spin Columns P30 (Biorad). The labeled OVA samples were combined with either sHsp S121C or sHsp E102C cages using a 5:1 molar ratio. The proteins were combined, vortexed, and reacted 1 h at room temperature and overnight at 4 °C. The final sHsp concentration was 2.34 mg/mL and the OVA concentration was 11.72 mg/mL in a total volume of 45 μL for each reaction. These reactions were repeated using a 20-fold excess of each SM(PEG)$_n$ linker (SM(PEG)$_2$, SM(PEG)$_6$, or SM(PEG)$_{12}$) from a stock solution of 250 mM to label the OVA.

Prior to conjugation, lysines on sHsp G41C were reacted with 50-fold molar excess of SPDP (Thermo Scientific) per sHsp subunit by the addition of 500 mM SPDP in DMSO to 2 mL of protein at 2.61 mg/mL. This reaction was stirred for 90 min at room temperature, and the labeled sHsp was purified by Superose 6, and stored at 4 °C overnight. For these reactions, a seven-fold molar excess of TCEP (Invitrogen) was added to the sHsp-SPDP (above) to reduce the SPDP, and this reaction was left for 30 min at room temperature to reduce the disulfides on the linker. UV–visible spectroscopy was used to monitor the completeness of the reaction as indicated by increasing absorbance at 324 nm corresponding to the thiopyridone product [42]. This sulfhydryl functionalized sHsp was reacted with OVA (80 μL, 7.72 mg/mL) samples labeled with a 2-fold or 20-fold molar excess of each SM(PEG)$_n$ linker (SM(PEG)$_2$, SM(PEG)$_6$, or SM(PEG)$_{12}$) using the protocol described above for the S121C and E102C reactions. The linking conditions for the sHsp G41C mutant combined with the OVA contained a final concentration of 30 mM TCEP. The final sHsp G41C and OVA concentrations were normalized to the conditions used with the other mutants: 2.34 mg/mL and 11.72 mg/mL respectively, in a total volume of 45 μL.

2.5. Synthesis and purification of the OVA–sHsp conjugate

A 250 mM stock solution of the commercially labeled cross-linking reagent SM(PEG)$_6$ (Thermo Scientific, Waltham, MA) was made in DMSO. The OVA was concentrated to 9.75 mg/mL, and 2.0 mL was reacted with a 2-fold molar excess of the linker, added dropwise to a vigorously stirring solution. The reaction was stirred for 40 min at room temperature, followed by immediate purification of the maleimide functionalized OVA from un-conjugated small molecule linker by Superose 6 size exclusion chromatography (GE Healthcare). Immediately after elution, the maleimide functionalized OVA was concentrated to approximately 13.4 mg/mL (using $E = 0.789\ (\text{mg/mL})^{-1}$) with a 10k MWCO Microcon filter (Millipore), and was mixed with sHsp S121C (2.62 mg/mL) for 1 h at room temperature followed by overnight at 4 °C.

A molar ratio of 5:1 OVA to sHsp was used to give final concentrations of 1.34 mg/mL OVA and 2.4 mg/mL sHsp within the linking reactions. Control reactions containing identical concentrations of sHsp or linker-labeled OVA alone were run in parallel. Free sulfhydryls on the proteins were then capped by reaction with 20-fold excess N-ethyl maleimide (Pierce) per sHsp subunit for 2 h at room temperature. The above procedure was repeated six times to obtain sufficient yield of the conjugated construct. Similar samples from these reactions were combined, spun down (5 min × 17,000 × g) to remove precipitate, and dialyzed into 25 mM triethanolamine (USB Corp, Santa Clara, CA) at pH 7.3.

The samples were purified by anion exchange chromatography on a MonoQ column (Amersham Pharmacia) using a linear gradient of 0 M to 500 mM NaCl in 25 mM triethanolamine at pH 7.3 (Fig. S1). Fractions corresponding to conjugated sample, sHsp and maleimide functionalized OVA were combined based on SDS-PAGE analysis of the fractions. The sHsp and maleimide functionalized OVA were mixed in a 5:1 molar ratio to obtain the mixed sample used for the *in vivo* experiments. All the samples were extensively dialyzed into 50 mM phosphate, 100 mM NaCl, and at pH 7.2 prior to *in vivo* experiments. The admixture of OVA and sHsp was comprised of equal microgram amounts of both sHsp (100 μg) and OVA (57 μg) (Sigma–Aldrich) as the conjugated form, and was suspended in sterile PBS.

2.6. Limulus amebocyte lysate assay

Prior to administration *in vivo* the endotoxin contamination for each protein preparation was determined using a limulus amebocyte lysate (LAL) assay (Associates of Cape Cod, Inc.; East Falmouth, MA). We determined that sHsp alone contained 1.3 μg LPS per dose, the OVA–sHsp conjugate contained 2.4 ng LPS per dose, the admixture of sHsp and OVA contained 3.4 ng LPS per dose, the P22 preparation contained 3 ng LPS per dose, and OVA alone contained 619 ng LPS per dose. A second batch of P22 was used for only Fig. 3B, with the following LAL results: The "LPS-high" P22 contained 8 μg LPS per dose, while the "LPS-low" P22 contained 14 ng per dose.

2.7. Confirmatory analysis

The size distribution of the VLPs was determined using dynamic light scattering (Brookhaven 90Plus particle size analyzer). For the Bradford assay, a series of protein standards was made using BSA (Sigma, A7906). One hundred microliters of Bradford Reagent (Amresco) was combined with 5 μL of each protein solution, and samples were incubated for 20 min, and the absorbance was measured at 315 and 605 nm. Samples were also run on 1 mm SDS-PAGE reducing gels (15% acrylamide for the running gel, 4% acrylamide for the stacking gel). The AlphaEaseFC software (Alpha Innotech) was used to identify bands and calculate the migration distances of species on the gels.

2.8. Western Blots

Proteins were transferred from the SDS-PAGE gels to Hybond C nitrocellulose membranes for 2 h at 200 mA. Membranes were blocked overnight with 5% milk and 0.01% Tween-20 in Tris-buffered saline, incubated with a 1:10,000 dilution of rabbit anti-OVA polyclonal antibody or rabbit anti-sHsp antibody (Millipore) for 3 h. The anti-sHsp antibody was purified from rabbit serum by ammonium sulfate precipitation. The membranes were incubated with a ratio of 1:5000 anti-rabbit antibody HRPO conjugate to blocking solution for 30 min, and blots were detected using an Opti-4CN kit (Biorad). Densitometry analysis was done using AlphaEaseFC software (Alpha Innotech).

2.9. Influenza virus

The influenza virus A/PR8/8/34 was produced at the Trudeau Institute, Saranac Lake, NY. Briefly, 10-day-old embryonated chicken eggs were infected for 72 h, and resultant allantoic fluid was recovered and stored at −80 °C until used.

2.10. Mice, pretreatment, and challenges

BALB/c, C57BL/6 or TLR4−/− mice were bred in-house at Montana State University, Bozeman, MT. At 6–8 weeks of age, male or female mice were enrolled in described experiments ($n = 5$ per group). In experiments utilizing intranasal pretreatments, 100 μg of sHsp (sHspG41C), or P22 were delivered in 50 μL volumes while the mice were lightly anesthetized under inhaled 5% isofluorane. Five pretreatment doses were delivered either daily for five days, or spaced evenly over the course of 2 weeks (both schedules

produced equivalent results). Importantly, we have extensively explored potential adverse side-effects on pulmonary function due to repeated sHsp administration, and have found none [5,34]. Pretreated mice were rested for 72 h, then challenged. In some experiments mice were challenged with the OVA–sHsp conjugate (sHspS121C), the OVA and sHsp (sHspS121C) admixture, OVA alone, or sHsp alone (sHspS121C), delivered i.n. in 100 μL volumes, again under light anesthesia. The OVA concentration (0.57 mg/mL), as determined by UV–visible spectroscopy, was held constant throughout groups, regardless of conjugation. For subcutaneous (s.c.) studies, no pretreatment was utilized. Instead, one s.c. dose of 100 μL OVA–sHsp, OVA with sHsp admixture, OVA with alum (10% $AlkSO_4$) admixture, alum alone (10% $AlkSO_4$), or OVA alone (0.57 mg/mL) were injected and antibody titers were measured over time. For influenza challenge studies, 1500 plaque forming units (pfu) A/PR8/8/34 influenza virus were delivered in 50 μL i.n. In experiments to determine the impacts of residual LPS, mice were similarly pretreated with "LPS-high" P22, "LPS-low" P22, an equal amount of LPS as in the "LPS-high" P22, or sterile pyrogen-free PBS in 50 μL i.n. All mice were then rested, and subsequently challenged with 100 μg sHspG41C in 50 μL i.n.

Mice were bled at relevant timepoints, and serum was separated from whole blood by centrifugation in separation tubes (Sarstedt; Germany). At indicated timepoints per experiment, mice were euthanized by intraperitoneal injection of sodium pentobarbital (90 mg/kg) and exsanguinated after no pedal response could be elicited. Mice were then lavaged with sterile PBS with 3 mM EDTA. BALF and sera were used to determine antibody titers by ELISA. In some experiments, lungs and tracheobronchial lymph nodes (TBLNs) were additionally collected and either homogenized through a wire mesh screen, or digested with agitation in 0.2% collagenase (Worthington Biochemical Corporation; Lakewood, NJ) with DNase (Sigma) at 37 °C for 1 h. Red blood cells were lysed from the lung homogenates using ACK lysis buffer, washed, resuspended in FcR block (clone 93), and stained for flow cytometry. Total cells from each tissue (BAL, lungs and TBLNs) were counted by hemocytometer. In some cases, whole lungs were instilled with OCT (SakuraFinetek; Torrance, CA), excised, and snap frozen in liquid nitrogen for histology. All animal procedures were pre-approved by Montana State University's IACUC. Experimental results were confirmed by at least two independent repetitions of similar design.

2.11. Immunostaining and flow cytometry

Frozen blocks were cut into 5 μM sections by cryostat (Leica Microsystems; Buffalo Grove, IL) and resultant lung sections were stained for expression of the polymeric Ig receptor (pIgR) with biotinylated goat anti-mouse pIgR (R&D Systems, Minneapolis, MN) followed by AF488-streptavidin (Invitrogen, Carlsbad, CA). Control sections were utilized to determine staining specificity. Images were acquired on a Nikon Eclipse E800 microscope (Nikon Instruments, Melville, NY) using Nikon NIS-Elements Imaging software.

Antibodies used for FACS staining of lung and TBLN homogenates included CD4 (GK1.5), B220 (RA3-6B2), Fas (Jo2), CXCR5 (2G8), CD138 (281-2), and streptavidin from BD Pharmingen; San Diego, CA; GL7 (GL7), and CXCR4 (2B11) from eBioscience; San Diego, CA; and ICOS (C398.4A) from Biolegend, San Diego, CA. FACS data was collected on a FACSCanto (BD) and FACS analysis was completed using FlowJo Software (Treestar, Ashland, OR). Briefly, forward and side scatter plots were gated on lymphocytes, as determined by size and granularity. Lymphocyte populations were then further analyzed for the expression of appropriate combinations of surface antigens, based off negative staining controls. Total cell numbers were then calculated based off total hemocytometer cell counts for each tissue.

2.12. ELISA

Serum and BALF antibodies levels were determined by ELISA. Briefly, high-binding polystyrene plates (Corning; Corning, NY) were coated and incubated with antigen (OVA, sHsp, or influenza virus membrane preparation) at 37 °C for 3 h, then moved to 4 °C overnight. Plates were washed with PBS with 0.05% tween, and blocked with nonfat dry milk. Serum samples were diluted at 1:100, and BALF samples were plated neat (from a 2 mL lavage) in duplicate. For influenza-specific ELISAs, samples were diluted in 2-fold dilutions to endpoint titer. All ELISAs were then incubated at 37 °C for 2 h. Plates were again washed and appropriate HRP-conjugated secondary antibodies (whole IgG, IgG1, IgG2a, IgG2b, IgG2c, IgG3, and IgA from SouthernBiotech, Birmingham, AL) were added and incubated for an additional 2 h at 37 °C. Finally, plates were again washed, developed using TMB substrate (Sigma–Aldrich), stopped with 1 M H_3PO_4, and read on a SpectraMax Plus plate reader (Molecular Devices; Sunnyvale, CA) at 450 nm. In some results, OVA-specific IgG was quantified using the mouse monoclonal antibody to OVA (Abcam, Cambridge, MA, ab17292).

2.13. Statistics

Statistical significance was determined by one-way ANOVA with a Bonferroni post-test of multiple comparisons, or in some cases an unpaired *t*-test was used. Significance was indicated by $^{*}p < .05$, $^{**}p < .01$, $^{***}p < .001$, or $^{****}p < .0001$. In some graphs (*) symbols are replaced by other symbols for clarity in comparison between multiple groups, but the number of symbols always corresponds to the appropriate *p*-value as described above for the asterisk, and explained in individual figure legends.

3. Results

3.1. Conjugation of OVA to sHsp

We carefully optimized conditions for the conjugation of the 45 kDa model antigen, ovalbumin (OVA), to the exterior surface of the sHsp. Our analysis revealed differences in conjugation efficiency dependent on the length of the small molecule linker, the stoichiometry of linker utilized, and the position of the reactive groups on the sHsp architecture. We chose conditions that provided the best yield of the conjugate product, while avoiding the formation of protein aggregates, to prepare the conjugated sample for *in vivo* experiments (see supplemental materials).

For preparation of the samples for administration to the lung, OVA was conjugated to the exterior of the sHsp S121C. A commercially available hetero-bifunctional cross-linking reagent $SM(PEG)_6$ was reacted with the lysines of OVA (Figs. 1 and S3A) to produce maleimide-functionalized OVA (Figs. 1Aii and S3B). Immediately following the labeling of OVA with $SM(PEG)_6$, unreacted small molecule linker was removed *via* size exclusion chromatography, and the maleimide-functionalized OVA (Fig. 1Aii) was reacted with sulfhydryl groups present on the sHsp S121C (Fig. 1Ai) to produce the OVA–sHsp conjugate (Fig. 1Aiii). Subsequent to conjugation, unreacted sulfhydryls on the sHsp S121C were capped by reaction with N-ethyl maleimide to inhibit disulfide formation, and the samples were further purified by anion exchange chromatography, which effectively separated free OVA from the sHsp S121C and OVA–sHsp conjugate (Fig. S1).

3.2. Characterization of the OVA–sHsp conjugate

The protein conjugates (OVA–sHsp) were detected on SDS-PAGE gels. As a comparison to the OVA–sHsp conjugate, samples containing sHsp, maleimide functionalized OVA, and an admixture of sHsp

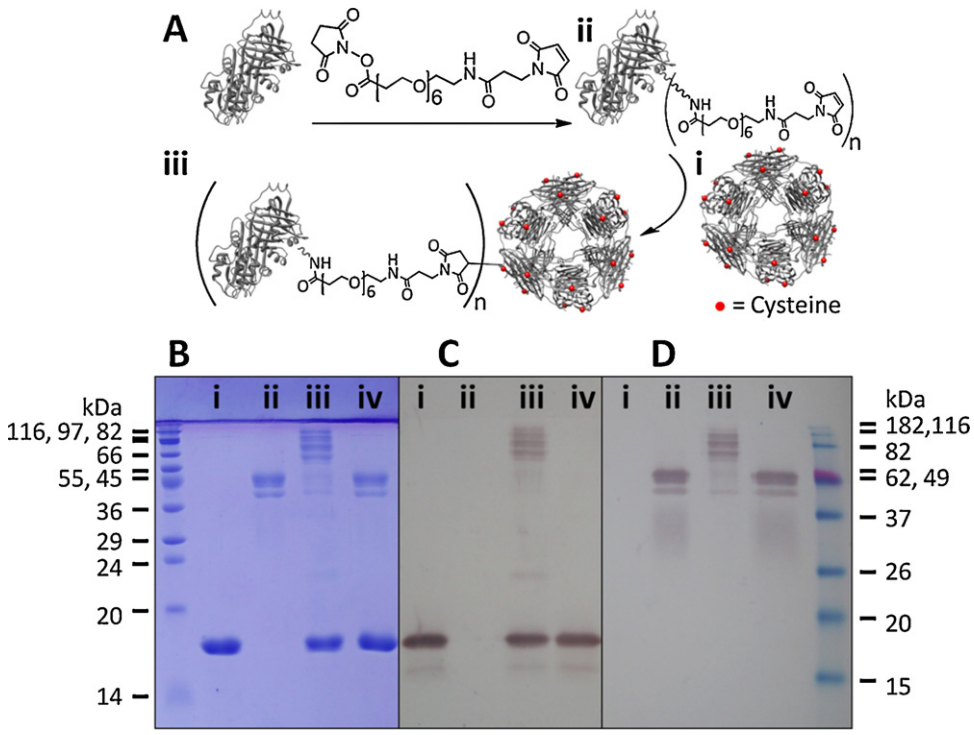

Fig. 1. OVA was conjugated to the sHsp S121C platform. The cross-linking methodology utilized to create the OVA–sHsp conjugate is shown (A). Ovalbumin was initially reacted with a commercially available crosslinking reagent, $SM(PEG)_6$, to produce a maleimide functionalized OVA (Aii) with *n* number of linkers attached. The functionalized OVA was reacted with sufhydryls on the sHsp S121C cage (Ai) to yield an OVA–sHsp conjugate (Aiii). The samples used for *in vivo* administration were analyzed by SDS-PAGE (B), and Western Blots with detection for either sHsp (C) or OVA (D). The lanes for each panel correspond to: sHsp S121C (i), OVA (ii), OVA–sHsp conjugate (iii), and an unlinked admixture (iv) of sHsp S121C (i) and OVA (ii).

and OVA were prepared. The admixture was prepared in a ratio of 5 OVA per 1 sHsp cage, and the OVA concentration within each sample was normalized to 0.57 mg/mL by UV–visible spectroscopy. The sHsp oligomeric complex dissociates into subunits under SDS-PAGE conditions, and a corresponding protein band (16.5 kDa) migrated close to the bottom of the gel (Fig. 1Bi). Also OVA appeared as two bands – whole OVA (45 kDa), and cleaved OVA (40.1 kDa) (Fig. 1Bii), as previously described [43]. Protein bands at higher molecular weights (>62 kDa) in Fig. 1Biii represented a polydisperse species of conjugated OVA–sHsp, and were later combined in total for use as the OVA–sHsp conjugate *in vivo* (further described below).

To determine if both OVA and sHsp were present in the upper bands of the sample in Fig. 1Biii, we performed Western Blot analysis using anti-sHsp (Fig. 1C) and anti-OVA (Fig. 1D) antibodies. Reactivity to both sHsp and OVA antibodies within the upper bands of the conjugated sample alone (Fig. 1Ciii and Diii) indicated the conjugation of OVA to sHsp. A semi-quantitative Western Blot (Fig. S4) suggested an average ratio of 2.6 OVA per sHsp cage within the conjugated sample. The total protein concentration of the conjugated (0.99 mg/mL), admixed (0.82 mg/mL), sHsp (0.61 mg/mL), and OVA (0.66 mg/mL) samples used for *in vivo* experiments were confirmed *via* Bradford assay.

The molecular weights of the bands corresponding to the OVA–sHsp conjugates were determined based upon their migration distance on SDS-PAGE gels (Figs. 1B and S5), and densitometry analysis (not shown). Protein bands corresponding to covalent conjugation between OVA and sHsp subunits on SDS-PAGE gel were identified by their presence within the conjugated sample (Fig. 1Biii) and absence within the sHsp (Fig. 1Bi), maleimide functionalized OVA (Fig. 1Bii), and the admixture (Fig. 1Biv) controls. We detected bands with calculated molecular weights of 58 and 62 kDa Fig. 1Biii and Fig. S5 that corresponded to the conjugation of a single sHsp subunit (16.5 kDa) to one cleaved OVA (40.1 kDa) or full length OVA (45 kDa), respectively. The upper bands detected between 67 and 84 kDa likely resulted from various forms of conjugation of OVA to sHsp (Fig. S5), and the smear of sample corresponding to molecular weights 85–150 kDa likely represented the conjugation of OVA to multiple sHsp subunits, as this entire smear reacted to both anti-OVA and anti-sHsp antibodies on a Western Blot. Thus, the resultant conjugated OVA–sHsp sample used for immunization was the culmination of a polydisperse species of OVA–sHsp, with varying degrees of multivalent array architecture.

We utilized size exclusion chromatography and dynamic light scattering measurements to probe the native state and size distribution of the particles within the samples used for immunization. The OVA–sHsp conjugate contained particles that were larger in size than those in the admixture, sHsp, or OVA. Size exclusion chromatography indicated that a distribution of larger species was present within the OVA–sHsp sample (Fig. S6) and by dynamic light scattering, the OVA–sHsp conjugate showed a larger average diameter than the maleimide functionalized OVA, sHsp S121C, or the admixture. The range of average diameters based on the intensity measurements on the samples repeated seven times were 6.0–9.9 nm for OVA, 15.1–17.3 nm for the admixture, 15.6–18.1 nm for sHsp S121C, and 29.9–41.0 nm for the OVA–sHsp conjugated sample (Fig. S7).

3.3. The immune response to OVA–sHsp is quick and intense after only a single intranasal dose

In our first *in vivo* studies we determined the potential of sHsp to serve as a novel vaccine delivery platform by its ability to facilitate the generation of antigen-specific immunity to OVA. Simultaneously, we determined how pretreatment of the lung

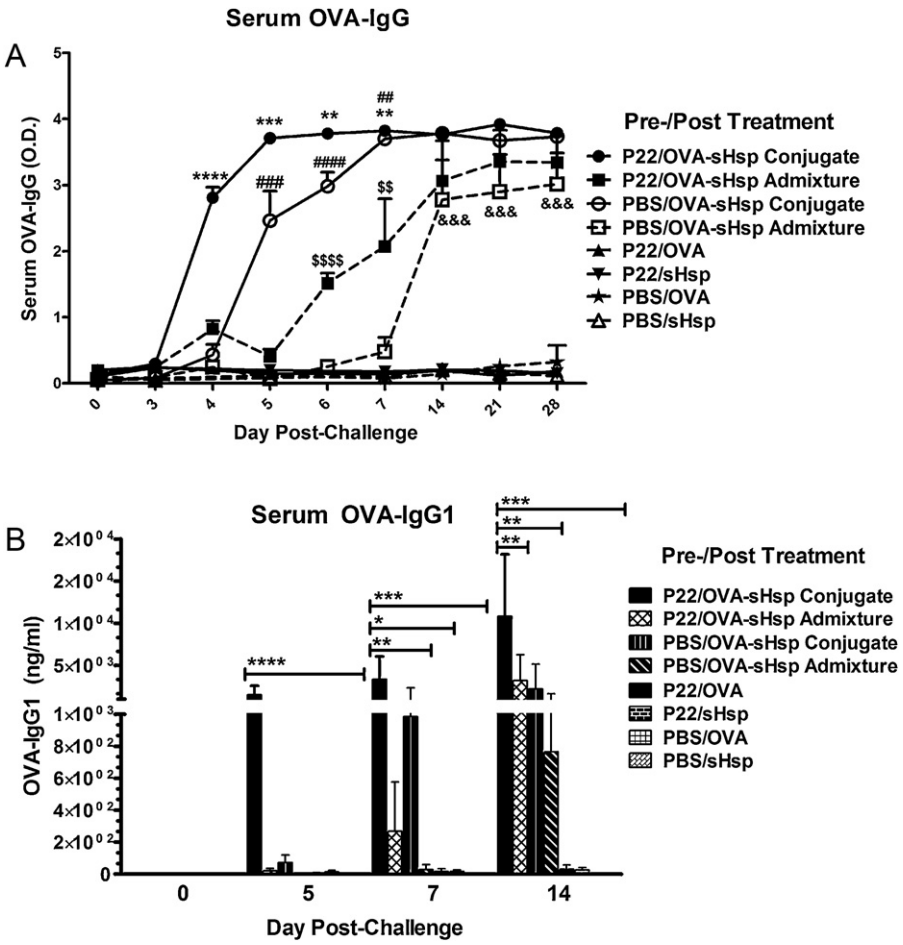

Fig. 2. The immune response to sHsp is accelerated and intensified after only a single intranasal dose. Mice were pretreated with P22 or vehicle (PBS), then challenged with the OVA–sHsp conjugate, the OVA and sHsp admixture, OVA alone, or sHsp alone. At indicated timepoints post-challenge, serum was collected and total OVA-specific IgG (A) or IgG1 (B) were determined by ELISA, and expressed as either O.D., or concentration (ng/mL). Results in this figure were compiled from two independent experiments with alternate days of serum collection. *Statistics*: In (A) (*) corresponds to the P22/OVA–sHsp conjugate group, (#) corresponds to the PBS/OVA–sHsp conjugate group, ($) corresponds to the P22/OVA–sHsp admixture group, and (&) corresponds to the top 4 traces as compared to the bottom four traces. In (B) the P22/OVA–sHsp conjugate group was evaluated against each other group and significance is indicated by (*).

with a heterologous VLP, P22, affects the subsequent response to antigen challenge. BALB/c mice were pretreated with either P22 or vehicle (PBS) intranasally (i.n.) in five doses and then allowed to rest for 72 h. Mice were then challenged with OVA conjugated to sHsp (OVA–sHsp), OVA and sHsp separately in solution (OVA–sHsp admixture), OVA alone, or sHsp alone. Serum was then collected at a range of timepoints post-antigen challenge for kinetic analysis. We found that mice which had received the P22 pretreatment, followed by a single dose of the OVA–sHsp conjugate, produced high amounts of OVA-specific serum IgG as early as 4 days post-challenge (Fig. 2A). This combination far outperformed any of the other treatment scenarios in both rapidity of antibody production and amount. Interestingly, the next highest antibody producing group, at early timepoints, was those mice that had also been challenged with the single dose OVA–sHsp conjugate, but had been pretreated with vehicle (PBS) only. This group also produced significantly higher antibody titers than the remaining combinations, although the response was delayed by about one day, as compared to those mice which had received P22 pretreatment (P22/OVA–sHsp conjugate). The remaining groups however, did not achieve the same peak titers until day 14 post-challenge, if at all, and equal early responses were delayed by 3–4 days (P22/OVA–sHsp admixture) or more (PBS/OVA–sHsp admixture), as compared to the P22/OVA–sHsp conjugate group. This indicated that the OVA–sHsp conjugate is immunologically recognized differently than is the admixture, and further that this resulted in accelerated antibody production.

We also determined the absolute concentration of the OVA-specific IgG1 response to the same pre- and post-treatment combinations (Fig. 2B). Consistent with our other results, mice that were pretreated with P22, then challenged with the OVA–sHsp conjugate, produced OVA-specific serum IgG1 in significant levels by day 5, and the quantities increased over the next nine days. Second best at producing high quantities of antibodies were both those mice which had received the control (PBS) pretreatment, but had been challenged with the OVA–sHsp conjugate, and those mice which had been pretreated with P22, then challenged with the sHsp and OVA admixture, which were measurable by day 7 post-challenge. Again, by day 14 post-challenge, the amounts of OVA-specific IgG1 were converging in only those groups in which the sHsp was delivered with OVA. Importantly, two additional conditions further heightened and accelerated the initiation of antibody production—heterologous VLP pretreatment with P22, and the physical conjugation of OVA to sHsp. While we will further discuss the impacts of pretreatment on subsequent challenge, we have demonstrated here that we can elicit an accelerated and intensified immune response to a weak antigen, in a single dose, by covalently conjugating it to sHsp.

3.4. The conjugation of an antigen to sHsp results in the generation of the same immune response to that antigen as sHsp itself

We have previously demonstrated that the priming of the lung with sHsp elicits an enhanced immune response to a subsequent pathogen challenge [5]. However, we had yet to define the immune response to sHsp itself. Therefore to determine the rate and intensity of the sHsp-specific antibody response we again pretreated mice intranasally with P22, or vehicle. Mice were then rested for 72 h, and challenged with the OVA–sHsp conjugate, the OVA and sHsp admixture, OVA alone, or sHsp alone. We then evaluated the sHsp-specific serum antibody response over 14 days post-challenge (Fig. 3A). We found that after only one challenge dose, all mice exposed to sHsp generated strong sHsp-specific IgG1 responses, which peaked as early as day 5 post-challenge in mice which had been pretreated with P22. Mice that did not receive P22 pretreatment were again two days delayed in the production of similar amounts of sHsp-specific antibody. However by day 7 post-challenge, all groups (except control OVA-only challenged mice) had generated similar levels of systemic sHsp-specific IgG1 in response to a single intranasal dose of sHsp antigen. Thus, the above-described OVA-specific response (Fig. 2) mirrors the accelerated kinetics of the sHsp-specific response, indicating that sHsp facilitates a carrier effect that results in an immune response to OVA that is similar to the response to the sHsp in both onset of antibody production and quantities produced.

Because our samples were purified from an *E. coli* expression system, we examined whether or not the heightened antibody responses observed were amplified by the residual LPS contained in our VLPs. We pretreated mice with either "LPS-low" P22, "LPS-high" P22, an equivalent amount of LPS as contained in the "LPS-high" P22 preparation, or sterile pyrogen-free PBS in five daily intranasal doses, as above. Mice were then challenged with sHsp alone, and serum was collected over 8 days to evaluate total anti-sHsp IgG. Importantly, we found that both "LPS-low" and "LPS-high" P22 elicited an equally enhanced early antibody response to the heterologous VLP challenge, while mice which were pretreated with LPS did not (Fig. 3B). In addition, we pretreated TRL4−/− or C57BL/6 mice with sHsp or PBS and challenged all mice with high-dose influenza virus. Importantly, only those mice that had been pretreated with sHsp were protected from influenza-induced body weight loss, regardless of their ability to respond to LPS (Fig. S2). These results indicated that the observed heightened immunity in VLP pretreated mice was not dependent on contaminating LPS.

3.5. sHsp can act as an adjuvant in the lungs

Next, to determine how the addition of sHsp, either delivered as a conjugate or an admixture with OVA, could act as an adjuvant for the immune response in the lungs, we pretreated mice with PBS only, and subsequently challenged them with the OVA–sHsp conjugate, admixture, or OVA alone, as described above. At day 7 post-challenge, we determined the level of OVA-specific serum IgG subclasses, and found that both the conjugated and admixture preparations of OVA elicited high-titer serum antibody O.Ds., while no such response to OVA alone was seen (Fig. 4A). Interestingly however, the OVA–sHsp conjugate promoted accelerated class-switching to IgG2a, IgG2b and IgG3 while only IgG1 was significantly detected for the admixture. To further determine the early events of isotype switching, we pretreated mice with either sHsp or vehicle, and challenged with the OVA–sHsp conjugate, or admixture. At days 0, 4, and 6, serum was collected and the OVA-specific IgG subclasses were determined by ELISA. We found that OVA-specific total IgG and IgG1 production was quicker by about two days in mice that had been pretreated with sHsp and challenged with the conjugated OVA–sHsp (Fig. 4B and C) as compared to the other treatments. The early IgG1 response in this group then translated into an enhanced production of class-switched IgG2a and IgG2b at day 6 post-challenge (Fig. 4D and E). This extent of isotype switching was not fully realized in any other group. Interestingly however, the enhanced class-switching capacity appeared to be more dependent upon the structure of the challenge antigen (OVA–sHsp conjugate *vs.* admixture) than the pretreatment with sHsp. Mice which had received only PBS pretreatment and had been challenged with the OVA–sHsp conjugate generated significantly higher IgG1, 2a, 2b, and IgG3 titers at day 6 post-challenge than those which were challenged with the admixture of sHsp and OVA (Fig. 4C–E and G). Very little IgG2c was produced at any timepoint (Fig. 4F). Thus, sHsp acts as an adjuvant when mixed with OVA and acts as a carrier when conjugated to OVA, resulting in unexpectedly potent antibody titers as early as 4 days after a single immunization in naïve mice.

Because we found that sHsp is a strong mucosal adjuvant, we next determined if sHsp would elicit a similar response when delivered to a non-mucosal site. We subcutaneously (s.c.) injected naïve mice with either the OVA–sHsp conjugate, the OVA and sHsp admixture, OVA alone, or OVA with its classical adjuvant–alum. We then determined the resultant serum antibody responses and found that when conjugated to antigen, sHsp acts as a strong adjuvant to OVA to produce an accelerated OVA-specific antibody response as early as day 5 post-challenge, while OVA–alum responses are delayed by two days comparatively (Fig. 4H). Again, the OVA and sHsp admixture elicited high titer antibody responses, as did the OVA and alum admixture, however, these combinations required more time to produce similar results. Taken together, sHsp conjugated to antigen acts as a carrier and elicits an accelerated antibody response to that antigen when delivered to several immunologically distinct sites.

3.6. sHsp-treatment induces local IgA responses

Growing recognition of the importance of site-specific immunity at mucosal surfaces [7], as well as tailoring immune responses per tissue [44–47] led us to determine whether pretreatment with sHsp or the conjugation of sHsp to OVA affects local IgA production. After pre-treatment with sHsp or PBS, and challenge with either the OVA–sHsp conjugate or the admixture, lung lavage fluids contained high levels of mucosal IgA and IgG in only those mice pretreated with sHsp (Fig. 5A and B). Local IgG production was further enhanced by the conjugation of sHsp to OVA (Fig. 5B). Notably, while many of our results demonstrate that the admixed OVA and sHsp preparation does not elicit the same enhancement as the conjugate, here, the admixture is equally potent in initiating mucosal IgA responses (Fig. 5A). sHsp thus serves a dual role—first as an immunomodulatory agent during pretreatment, and second, as an adjuvant for specific antigens. Furthermore, we found that the pretreatment of the lung with sHsp caused an upregulation of the polymeric Ig receptor (pIgR) on lung epithelial cell surfaces prior to antigen challenge (Fig. 5C). Thus, the capacity for the release of local secretory IgA into the airway lumen is enhanced by sHsp pretreatment.

3.7. sHsp pretreatment of the lungs enhances influenza-specific antibody responses and changes the lung environment, making it more conducive to local antibody responses

We have previously shown that sHsp pretreatment of mice subsequently infected with influenza, accelerates the onset and intensity of an influenza-specific IgG response similar to how sHsp pretreatment enhances the antibody response to OVA–sHsp [5]. We then determined whether sHsp pretreatment also affected the

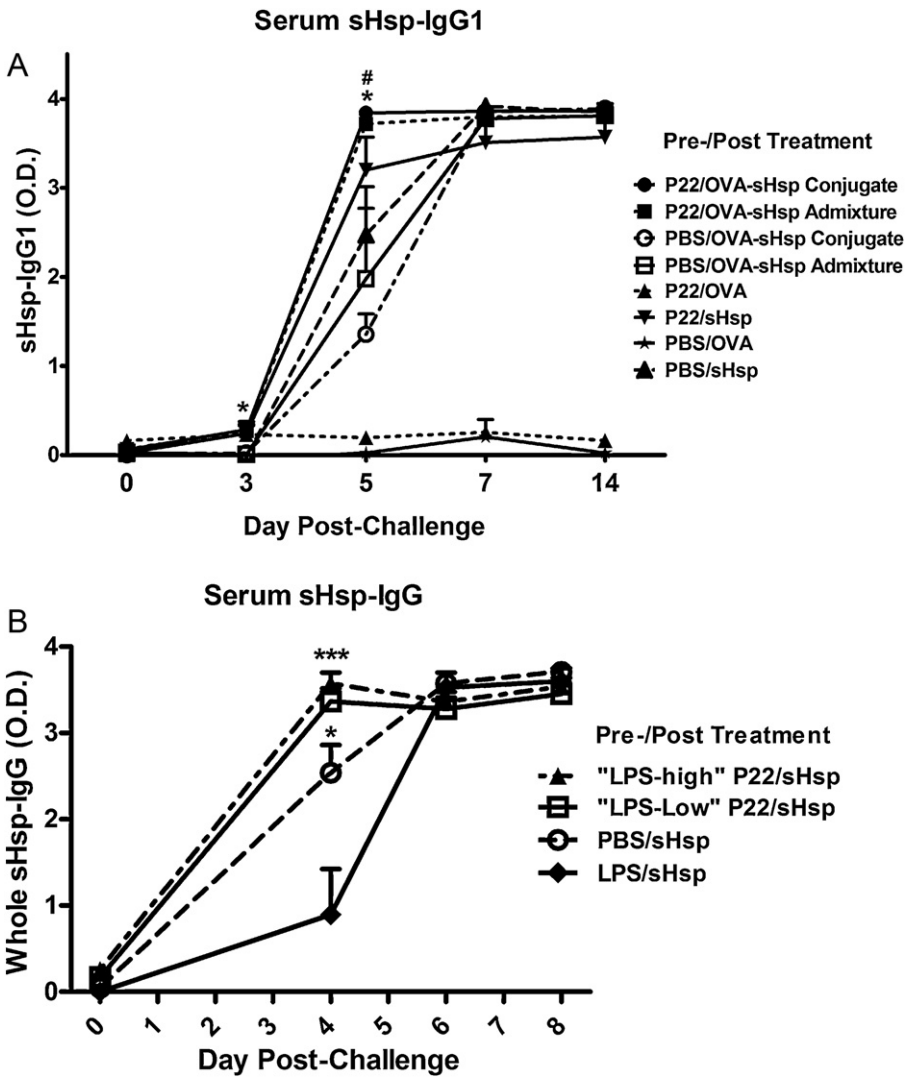

Fig. 3. The conjugation of an antigen to sHsp results in the generation of the same immune response to that antigen as sHsp itself. In (A) mice were pretreated with P22 or vehicle (PBS) i.n. All mice were then challenged with either the OVA–sHsp conjugate, OVA and sHsp admixture, sHsp alone, or OVA alone. At indicated times, serum was collected and sHsp-specific IgG1 was measured by ELISA (A). In (B) mice were pretreated with "LPS-high" P22 (8 μg LPS per dose), "LPS-low" P22 (14 ng LPS per dose), an equivalent amount of LPS alone (8 μg per dose), or sterile pyrogen-free PBS in five doses i.n. All mice were then challenged with 100 μg sHsp and whole serum IgG to sHsp was determined over 8 days (B). *Statistics*: In (A), at day 3, the P22/OVA–sHsp conjugate group (*) had significantly higher levels of antibody than the PBS/sHsp group only. At day 5, the P22/OVA–sHsp conjugate group had significantly higher levels of antibody than both the PBS/OVA–sHsp conjugate (**) and PBS/OVA–sHsp admixture (*) groups. Additionally, the P22/OVA–sHsp admixture and P22/sHsp groups had significantly higher levels of antibody than the PBS/OVA–sHsp conjugate group (## and #, respectively). In (B) at day 4 all groups had produced significantly more antibody than the LPS pretreated group where both P22 groups ("LPS-high" and "LPS-low") were *** $p < .001$, and PBS was * $p < .05$ comparatively to the LPS group.

kinetics of antibody class switching after influenza infection as it does with OVA–sHsp. In mice pretreated with sHsp or control, then challenged with 1500 pfu mouse-adapted PR8 (H1N1) influenza virus, we determined the corresponding endpoint-dilution titer of influenza-specific IgG subclasses in the local BALF, and found that, as had been expected due to the OVA results, influenza-specific BALF IgG was enhanced both in titer and in the rate of class-switching in mice which had been exposed to sHsp prior to infection (Fig. 6A–F). Thus, sHsp pretreatment similarly affects antibody responses to a model antigen and a pathogen-associated antigen.

We next determined how sHsp pretreatment modulates the lung environment. We pretreated mice with sHsp, then challenged with influenza. We found that sHsp pretreatment stimulated the formation of germinal centers (GC) in the lung and enlarged GC B cell areas in the tracheobronchial lymph node (TBLN) (Fig. 7A and B). In both tissues, GC B cells were more prevalent by at least one log in sHsp-primed mice before infection, indicating that the microenvironment within the lung and local lymph node had been stimulated to adjust to the current antigenic exposure. We also found that T follicular helper (T_{FH}) cells were more abundant in both the lungs and TBLNs of sHsp-primed mice (Fig. 7C and D). Thus, germinal center reactions were more easily facilitated within the lungs and local lymph nodes of sHsp-primed mice. Over the course of infection, a clear advantage in GC organization and establishment was observed as both GC B cells and T_{FH} cells retained significantly higher numbers in sHsp-primed mice as opposed to controls. Thus, highly active GC reactions, complete with T_{FH} cell help, were likely facilitating the enhanced antibody isotype switching and elevated antibody production.

Given that GC's are enhanced, we also stained for the presence of plasma cells, as defined by their lymphocyte size and

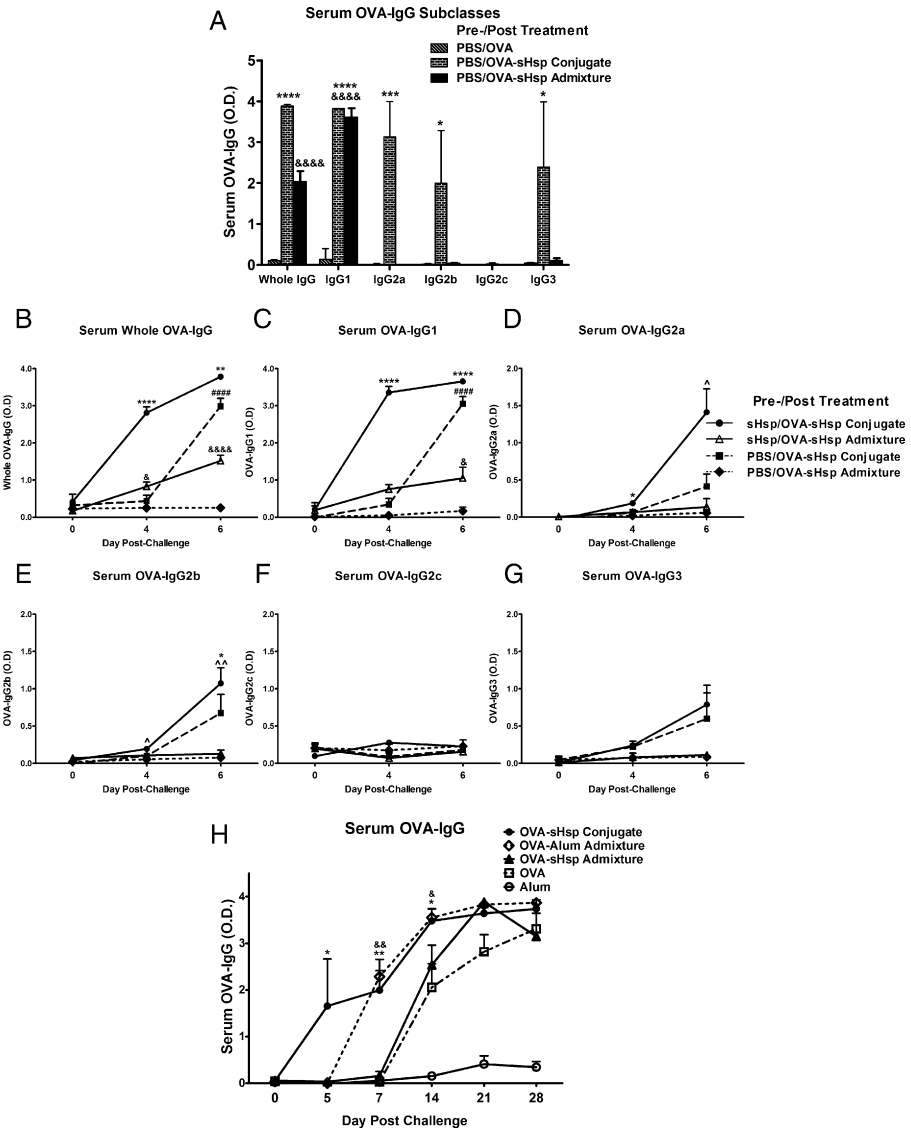

Fig. 4. sHsp can act as an adjuvant in the lungs. In (A), all mice were pretreated with PBS i.n., and then challenged with the OVA–sHsp conjugate, OVA and sHsp admixture, or OVA alone. Serum IgG subclass titers were then determined by ELISA at day 7 post-challenge. In (B)–(G), mice were pretreated with either sHsp or vehicle (PBS) i.n., then challenged with the OVA–sHsp conjugate, or the OVA and sHsp admixture. At days 0, 4, and 6 serum was collected and total OVA-specific IgG subclasses were determined by ELISA. In (H), mice were not pretreated, but were challenged s.c. with the OVA–sHsp conjugate, OVA and sHsp admixture, OVA and alum, OVA alone, or alum alone. Serum was then collected over 28 days, and OVA-specific serum IgG was determined by ELISA. *Statistics*: For (A) (*) denote the PBS/OVA–sHsp conjugate group as compared to the PBS/OVA–sHsp admixture group and OVA alone and (&) denotes the PBS/OVA–sHsp admixture group as compared to OVA alone. For (B)–(C) symbols are used per line to indicate significance over all other groups. In (D) (∧) represents that the sHsp/OVA–sHsp conjugate group is significant as compared to the PBS/OVA–sHsp admixture group, but not the PBS/OVA–sHsp conjugate group at day 6. And in (E), at days 4 and 6 (∧) indicates that the sHsp/OVA–sHsp conjugate group was significant over the PBS/OVA–sHsp admixture group, and was also significant over the PBS/OVA–sHsp conjugate group (*) at day 6 only. For (H) at day 5 (*) denotes that the OVA–sHsp conjugate group was significant as compared to the OVA–alum admixture. At day 7, both the OVA–sHsp conjugate group (*) and the OVA–alum admixture group (&) were significant as compared to the remaining groups. At day 14 both the OVA–sHsp conjugate group (*) and the OVA–alum admixture group (&) were significant as compared to the OVA alone group. Significance was not denoted for differences against alum alone.

morphology, loss of B220 and CD19, with or without CD138 (syndecan) expression, and the upregulation of CXCR4 (Fig. 7E and F). Interestingly, we found that in the lung, plasma cells at day 0, assumedly secreting antibody against sHsp, were markedly more abundant in primed mice. However, the number of cells present rapidly declined over the course of the influenza infection, which may represent profound plasticity in the specificity of the inhabitants of GC areas of the lung (as has been described by others) [48]. In the TBLN, plasma cells were again more numerous before infection in the sHsp-primed mice. However, here, they remained elevated as compared to control mice until the resolution of infection, at which point the plasma cell numbers in the TBLNs of both groups converged. Unlike the lung however, similar trends were followed by both groups in the TBLN. We surmise from this data that sHsp-specific plasma cells in the lung are decreasing, while simultaneously, influenza-specific plasma cells are increasing. Therefore, due to the likely variable rates of influx and efflux, we may not have exclusively quantified the rate of increase in influenza-specific plasma cells due to sHsp priming. What remains puzzling however is how sHsp-specific germinal centers and plasma cells become influenza- or OVA-specific at an accelerated rate when compared to control mice. Given our experimental data, we surmise, as have others [2], that the pulmonary microenvironment adjusts in the context of innate, humoral, and cellular immune responses in reaction to the menagerie of antigenic exposures encountered, which are unique to that individual. Thus, sHsp pretreatment significantly enhances the efficiency of future immune responses.

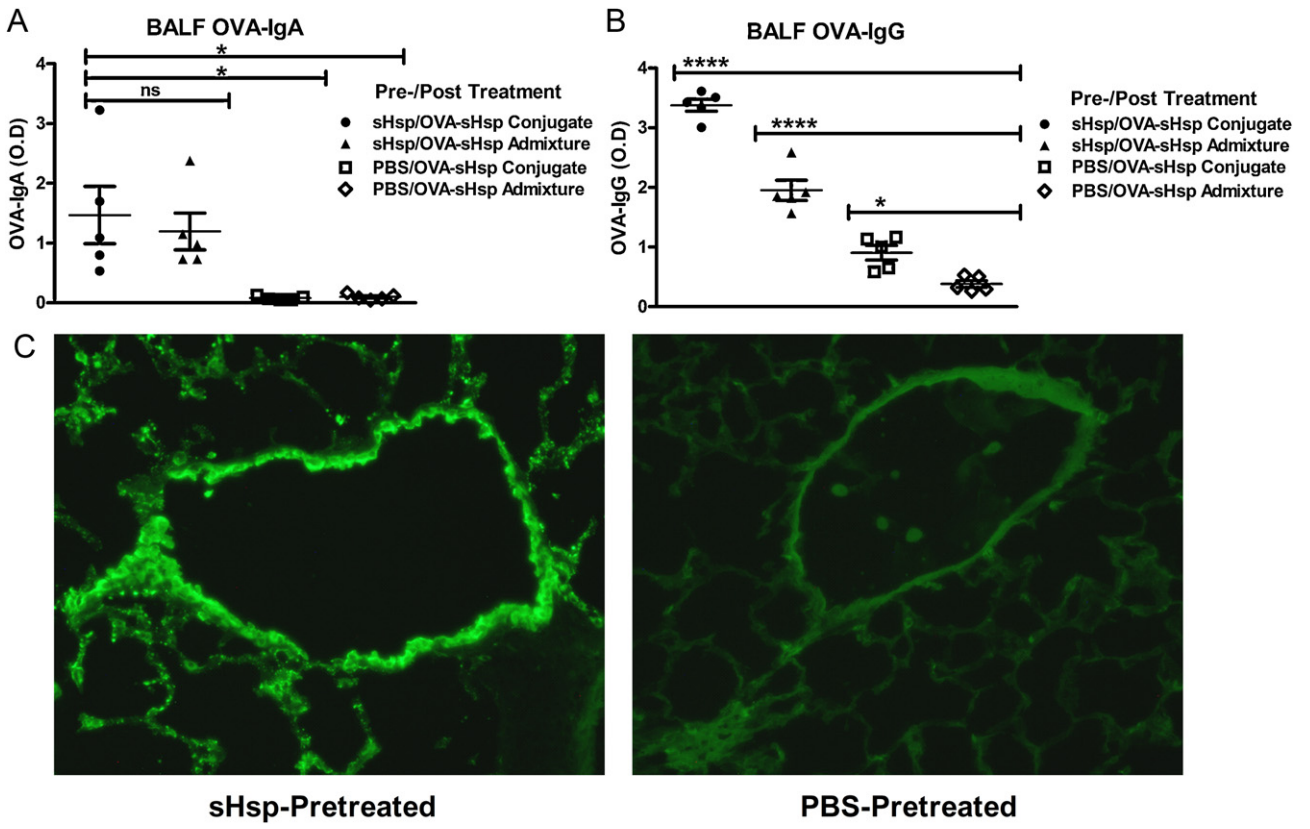

Fig. 5. sHsp treatment induces local IgA responses. Mice were pretreated with sHsp or vehicle control (PBS) i.n., then challenged with the OVA–sHsp conjugate, or the OVA and sHsp admixture. In (A) and (B), BALF OVA-specific IgA and IgG were measured at day 7 post-challenge by ELISA. In (C), frozen lungs were sectioned and stained for the presence of the polymeric Ig receptor in either sHsp- (left) or vehicle-primed (right) mice. *Statistics*: For (A) the sHsp/OVA–sHsp conjugate was significant as compared to both PBS pretreated groups. In (B) the sHsp/OVA–sHsp conjugate was significant as compared to all the below groups, as was the sHsp/OVA–sHsp admixture, and the PBS/OVA–sHsp conjugate.

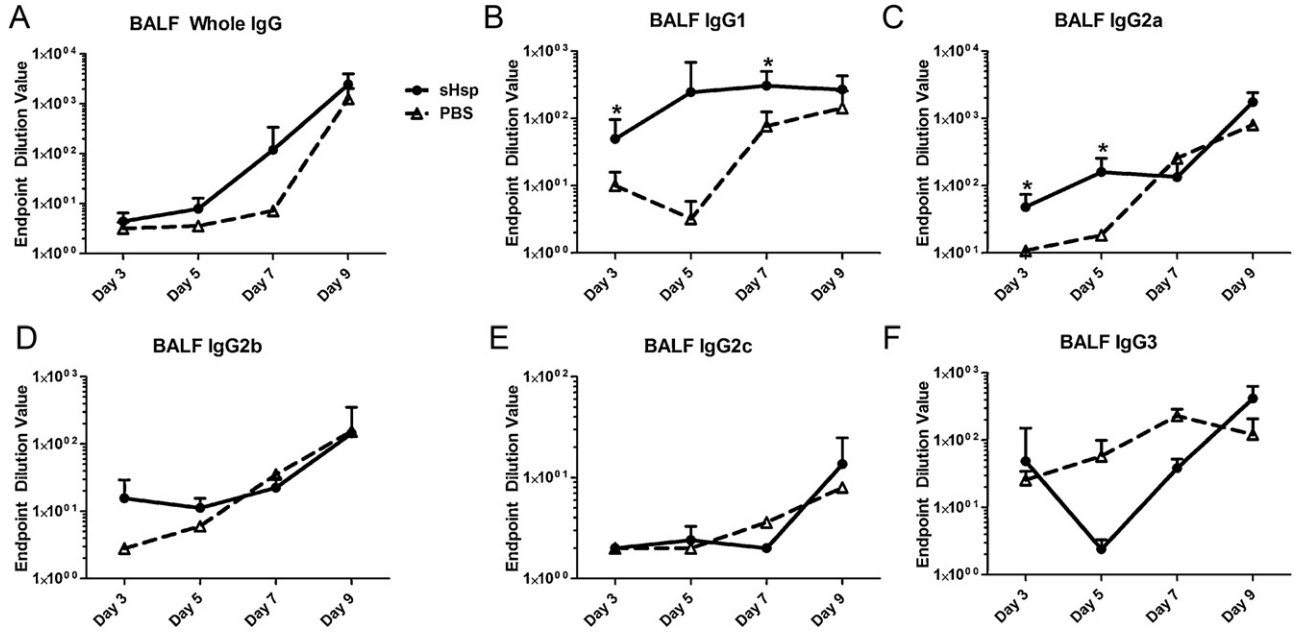

Fig. 6. sHsp pretreatment accelerates the onset of influenza-specific IgG in BALF. Mice were pretreated with either sHsp or vehicle (PBS), and challenged with 1500 pfu PR8 influenza i.n. At indicated times post-challenge, mice were sacrificed and lavaged. Influenza-specific whole IgG (A), IgG1 (B), IgG2a (C), IgG2b (D), IgG2c (E), and IgG3 (F) in the BALF were determined to endpoint titer in 2-fold dilutions by ELISA.

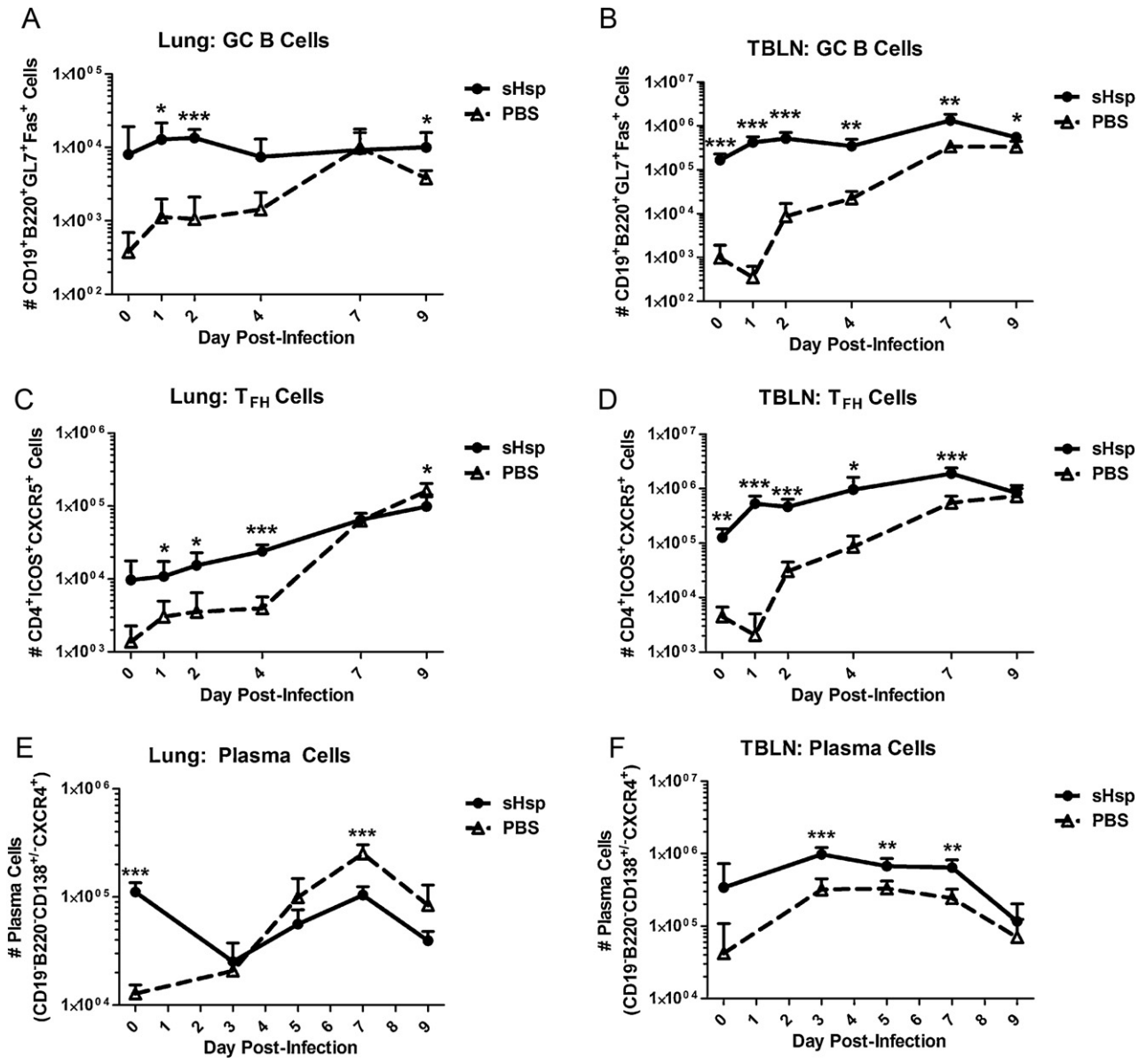

Fig. 7. sHsp pretreatment of the lungs leads to an even faster response to subsequent antigens. Mice were pretreated with sHsp or vehicle (PBS) i.n., infected with 1500 pfu PR8, and then sacrificed at indicated times post-infection. Lungs and tracheobronchial lymph nodes (TBLNs) were homogenized and stained for germinal center (GC) B cells (A and B), T follicular helper cells (TFH) (C and D), or plasma cells (E and F) and total cell numbers were quantified by FACS and cell counts.

4. Discussion

We have shown previously that sHsp pretreatment induces pulmonary changes that protect against a subsequent challenge with a variety of pathogens, and additionally sHsp pretreatment decreases tissue damage, while accelerating viral clearance [5]. We demonstrate here that both sHsp pretreatment, and the conjugation of sHsp to an antigen of interest, provided enhanced immunity, by likely distinct immunological mechanisms. Pretreatment with sHsp elicited the organization of GCs in the lungs and TBLNs, which then functioned to accelerate and intensify the onset of antibody production. Most importantly, pre-priming of the lung with sHsp elicited an enhanced mucosal IgA response, and the upregulation of epithelial pIgR. This response is not dependent upon the physical conjugation of OVA to sHsp, as the OVA and sHsp admixture elicited IgA production equally well. For local BALF IgG production, however while sHsp pretreatment seemed to be the factor majorly responsible for the enhanced antibody titers, the conjugation of sHsp to OVA also contributed. Finally, heterologous VLP pretreatment was equally efficient at eliciting heightened immunity, as demonstrated with P22 pretreatment followed by OVA–sHsp challenge, and sHsp pretreatment followed by influenza challenge. While heterologous immunity has been extensively described in both the context of cross-protective immunity, and inappropriate or harmful skewing, the underlying mechanisms are still incompletely defined [1–3,48–51]. We demonstrate here that pretreatment of mice with non-pathogenic VLPs stimulated immunity through some type of priming, which resulted in a subsequent enhanced response to OVA, and furthermore, facilitated pathogen clearance and decreased damage in response to viral challenge (Figs. 5 and 6 and Ref. [5]).

In addition to pretreatment, we also demonstrate the utility of sHsp as a novel vaccine platform through the direct conjugation to an antigen of interest. In contrast to the conjugation of antigenic peptides to a multivalent scaffold, we present the conjugation of an entire protein antigen to the protein cage surface for *in vivo*

application. Through this approach, it is possible for the conjugated antigen to be seen by the immune system as part of the VLP, and elicits a response similar to that the VLP elicits. As previous work has demonstrated that chemical conjugation efficiency of large unrelated proteins to a viral capsid is inhibited as the size of the protein is increased [38], conditions for the chemical conjugation of the 45 kDa OVA to the sHsp cage were optimized for these proteins. We observed that the attachment position on the sHsp cage, the length of the chemical linker, and the stoichiometry of linker labeling affected the conjugation efficiency.

When delivered as an OVA–sHsp conjugate, sHsp acted to enhance OVA-specific early antibody production. Thus, sHsp acted as a carrier, causing the OVA-specific response to mirror the sHsp-specific response in onset of antibody production and quantity produced. Interestingly, while we have utilized sHsp in two scenarios, as a pretreatment, or a vaccine delivery platform, and these scenarios likely are working through distinct immunostimulatory mechanisms, the activities of each are not mutually exclusive, and can in fact, synergize—as the antibody responses to the conjugated OVA–sHsp are enhanced by the pretreatment with either sHsp or P22.

While we have yet to define the exact cellular receptors responsible for signal transduction to initiate the immune response to the VLPs, we hypothesize that the repeating subunits of sHsp or P22 allow for the ability to crosslink or otherwise engage single or multiple cellular receptor domains. And as it has been suggested by others, cell surface integrins on antigen-presenting cells likely play a role in recognizing viral capsids [22,23,25]. Targeting evolutionarily conserved domains therefore facilitates plasticity in this delivery system, allowing for the utilization of sHsp conjugation with other antigens—especially those which have complicated or precluded the design and manufacture of potent vaccines. Additionally, the complex geometry of the OVA–sHsp conjugate may be impacting the resultant immune responses observed. It has been well demonstrated that the specific geometric display of multivalent antigens significantly heightens immune responses [20,52,53], and especially B cell recognition [52,54–56], and further, that such displays may even provide enough co-stimulation to break tolerance to self-antigens without the need for adjuvants [55,57]. Thus the arrangement of the OVA–sHsp conjugate may explain the enhanced class-switching which we observed only in those mice which received the conjugated form of OVA–sHsp (Fig. 4A–G). We therefore demonstrate the utility in displaying a poorly immunogenic antigen as a multivalent array through the conjugation to a VLP platform to elicit enhanced specific immunity.

Furthermore, the implications for a single-dose vaccine that accelerates the antibody response to antigens, producing high titer antibody within 4–7 days of primary immunization holds significant clinical potential. In this regard, new strategies which employ post-exposure prophylaxis represent an arguably greater demand than pretreatment, as we continually lose antibiotic options due to the emergence of resistant strains of bacteria, and are no better at predicting future viral outbreaks. Thus, we may be able to exploit sHsp, conjugated to an antigen of choice, to elicit early IgA responses. Importantly, few adjuvants currently on the market can be safely delivered to the lung, nor do they produce high titer, site-specific mucosal IgA [58].

We have presented a novel vaccine platform that is amenable to easy manipulation, facilitating flexibility and broad implications for vaccination strategies against many types of pathogens. This type of platform is especially noteworthy, as it may be utilized as an immunomodulatory agent alone (as in the case of pretreatments), for modifying the current state of immune homeostasis, or as a carrier and adjuvant for a defined antigen of interest. This phenomenon of immune homeostasis and skewing has been extensively described in terms of an individual's history of pathogen and allergen exposure [3,51]. However, to date few attempts to harness the potential of immune priming, with or without involving pathogen-specific epitopes or proteins, have been described [4]. Thus, we propose that we have identified an approach which utilizes strategies for priming against undefined broad-spectrum antigens, and also for delivering a highly efficacious single-dose vaccine against a defined antigen.

Importantly, we have additionally shown that the route of delivery (directly to the lung by intranasal instillation) results in the creation of an immune response that is specifically tailored to that tissue, and its individual requirements. While concern in purposely eliciting an immune response in the lung is justified, we and others [52] indicate here (and elsewhere [5]) that by doing so with VLPs, the power of tissue-specific immunity can be harnessed to provide a safe and appropriate response in the context of both the pathogen (sterilizing immunity), and the protection of lung function. Furthermore, the onset of immunity when the lung is pre-exposed to sHsp is accelerated, again indicating that the pretreatment with sHsp impacts the future, unpredictable pathogen challenge. In addition, we have previously shown that the deposition of VLPs in mouse lungs has no adverse effects and even attenuates lung hypersensitivity [5].

Virus-like particle and nanoparticle vaccination strategies are gaining recognition as the next class of safe and effective platforms. Notably, while many vaccines are expensive to produce, and require refrigeration, many types of VLPs and nanoparticles are stable, and easily preserved through freeze-drying, creating opportunities for distribution that may be otherwise precluded due to cost or logistics. Therefore, we have herein described a novel mucosal vaccination strategy that accounts for tissue-specificity, and exploits natural immunity to provide accelerated and enhanced antibody and cellular immune responses to primary antigen challenge.

Acknowledgments

We thank the Harmsen lab staff for technical assistance in experiments, Erin Dobrinen for LAL assay results, Abby Leary for immunostaining and microscopy, Ben Johnson and Suzanne Wilson for producing and purifying the sHsp and P22, Peter Previlege (University of Alabama, Birmingham) for providing the P22 expression vectors, and the staff of Montana State University's Animal Resource Center for animal care and technical aid. This work was made possible by funding from NIH/NIAID R56AI089458; the Rocky Mountain Research Center of Excellence (RMRCE) U54AI065357; NIH/NIAID R21AI083520; the IDea Network for Biomedical Research Excellence (INBRE) P20 RR016455 and P20GM103474; the Center for Zoonotic and Emerging Infectious Diseases (COBRE) P20 RR020185 and P20GM103500; NSF-CBET-0709358; the M.J. Murdock Charitable Trust, and the Montana State University Agricultural Experimental Station.

Appendix A. Supplementary data

Supplementary data associated with this article can be found, in the online version, at doi:10.1016/j.vaccine.2012.03.035.

References

[1] Selin LK, Brehm MA, Naumov YN, Cornberg M, Kim SK, Clute SC, et al. Memory of mice and men: CD8+ T-cell cross-reactivity and heterologous immunity. Immunol Rev 2006;211(June):164–81.
[2] Goulding J, Snelgrove R, Saldana J, Didierlaurent A, Cavanagh M, Gwyer E, et al. Respiratory infections: do we ever recover? Proc Am Thorac Soc 2007;4(December (8)):618–25.
[3] Kamradt T, Goggel R, Erb KJ. Induction exacerbation and inhibition of allergic and autoimmune diseases by infection. Trends Immunol 2005;26(May (5)):260–7.

[4] Walzl G, Tafuro S, Moss P, Openshaw PJ, Hussell T. Influenza virus lung infection protects from respiratory syncytial virus-induced immunopathology. J Exp Med 2000;192(November (9)):1317–26.
[5] Wiley JA, Richert LE, Swain SD, Harmsen A, Barnard DL, Randall TD, et al. Inducible Bronchus-associated lymphoid tissue elicited by a protein cage nanoparticle enhances protection in mice against diverse respiratory viruses. PLoS One 2009;4(9):e7142.
[6] Holt PG. Development of bronchus associated lymphoid tissue (BALT) in human lung disease: a normal host defence mechanism awaiting therapeutic exploitation? Thorax 1993;48(November (11)):1097–8.
[7] Pabst R, Tschernig T. Bronchus-associated lymphoid tissue: an entry site for antigens for successful mucosal vaccinations? Am J Respir Cell Mol Biol 2010;43(August (2)):137–41.
[8] Tschernig T, Pabst R. What is the clinical relevance of different lung compartments? BMC Pulm Med 2009;9:39.
[9] Holmgren J, Czerkinsky C. Mucosal immunity and vaccines. Nat Med 2005;11(April (4 Suppl.)):S45–53.
[10] Cox RJ, Brokstad KA, Ogra P. Influenza virus: immunity and vaccination strategies. Comparison of the immune response to inactivated and live, attenuated influenza vaccines. Scand J Immunol 2004;59(January (1)):1–15.
[11] Belshe R, Lee MS, Walker RE, Stoddard J, Mendelman PM. Safety, immunogenicity and efficacy of intranasal, live attenuated influenza vaccine. Expert Rev Vaccines 2004;3(December (6)):643–54.
[12] Nochi T. Nanogel antigenic protein-delivery system for adjuvant-free intranasal vaccines. Nat Mater 2010;9(7):572–8.
[13] Heegaard PMH. Dendrimers for vaccine and immunostimulatory uses. A review. Bioconjug Chem 2010;21(3):405–18.
[14] Stano A. PPS nanoparticles as versatile delivery system to induce systemic and broad mucosal immunity after intranasal administration. Vaccine 2010.
[15] Jegerlehner A. A molecular assembly system that renders antigens of choice highly repetitive for induction of protective B cell responses. Vaccine 2002;20(25–26):3104.
[16] Peacey M. Versatile RHDV virus-like particles: incorporation of antigens by genetic modification and chemical conjugation. Biotechnology and bioengineering 2007;98(5):968–77.
[17] Chen Z. Protective immune response in mice vaccinated with a recombinant adenovirus containing capsid precursor polypeptide P1, nonstructural protein 2A and 3C protease genes (P12A3C) of encephalomyocarditis virus. Vaccine 2008;26(4):573.
[18] Brennan FR. Chimeric plant virus particles administered nasally or orally induce systemic and mucosal immune responses in mice. J Virol 1999;73(2):930.
[19] Caldeira JC. Immunogenic display of diverse peptides, including a broadly cross-type neutralizing human papillomavirus L2 epitope, on virus-like particles of the RNA bacteriophage PP7. Vaccine 2010;28(27):4384.
[20] Manayani DJ. A viral nanoparticle with dual function as an anthrax antitoxin and vaccine. PLoS pathog 2007;3(10):e142.
[21] Jennings GT. The coming of age of virus-like particle vaccines. Biol Chem 2008;389(5):521–36.
[22] Lenz P, Day PM, Pang YY, Frye SA, Jensen PN, Lowy DR, et al. Papillomavirus-like particles induce acute activation of dendritic cells. J Immunol 2001;166(May (9)):5346–55.
[23] Lenz P, Thompson CD, Day PM, Bacot SM, Lowy DR, Schiller JT. Interaction of papillomavirus virus-like particles with human myeloid antigen-presenting cells. Clin Immunol 2003;106(March (3)):231–7.
[24] Savard C, Guerin A, Drouin K, Bolduc M, Laliberte-Gagne ME, Dumas MC, et al. Improvement of the trivalent inactivated flu vaccine using PapMV nanoparticles. PLoS One 2011;6(6):e21522.
[25] Lacasse P, Denis J, Lapointe R, Leclerc D, Lamarre A. Novel plant virus-based vaccine induces protective cytotoxic T-lymphocyte-mediated antiviral immunity through dendritic cell maturation. J Virol 2008;82(January (2)):785–94.
[26] Acosta-Ramirez E, Perez-Flores R, Majeau N, Pastelin-Palacios R, Gil-Cruz C, Ramirez-Saldana M, et al. Translating innate response into long-lasting antibody response by the intrinsic antigen-adjuvant properties of papaya mosaic virus. Immunology 2008;124(June (2)):186–97.
[27] Landry N, Ward BJ, Trepanier S, Montomoli E, Dargis M, Lapini G, et al. Preclinical and clinical development of plant-made virus-like particle vaccine against avian H5N1 influenza. PLoS One 2010;5(12):e15559.
[28] Roldao A, Mellado MC, Castilho LR, Carrondo MJ, Alves PM. Virus-like particles in vaccine development. Expert Rev Vaccines 2010;9(October 10):1149–76.
[29] Huang Z, Elkin G, Maloney BJ, Beuhner N, Arntzen CJ, Thanavala Y, et al. Virus-like particle expression and assembly in plants: hepatitis B and Norwalk viruses. Vaccine 2005;23(March (15)):1851–8.
[30] Kim KK, Kim R, Kim SH. Crystal structure of a small heat-shock protein. Nature 1998;394(August (6693)):595–9.
[31] Kim R, Kim KK, Yokota H, Kim SH. Small heat shock protein of *Methanococcus jannaschii*, a hyperthermophile. Proc Natl Acad Sci USA 1998;95(August (16)):9129–33.
[32] Flenniken ML, Willits DA, Harmsen AL, Liepold LO, Harmsen AG, Young MJ, et al. Melanoma and lymphocyte cell-specific targeting incorporated into a heat shock protein cage architecture. Chem Biol 2006;13(February (2)):161–70.
[33] Flenniken ML, Willits DA, Brumfield S, Young MJ, Douglas T. The small heat shock protein cage from *Methanococcus jannaschii* is a versatile nanoscale platform for genetic and chemical modification. Nano Lett 2003;3(11):1573–6.
[34] Kaiser CR, Flenniken ML, Gillitzer E, Harmsen AL, Harmsen AG, Jutila MA, et al. Biodistribution studies of protein cage nanoparticles demonstrate broad tissue distribution and rapid clearance in vivo. Int J Nanomed 2007;2(4):715–33.
[35] Liepold LO. Supramolecular protein cage composite MR contrast agents with extremely efficient relaxivity properties. Nano Lett 2009;9(12):4520–6.
[36] Abedin MJ, Liepold L, Suci P, Young M, Douglas T. Synthesis of a cross-linked branched polymer network in the interior of a protein cage. J Am Chem Soc 2009;131(12):4346–54.
[37] Gupta SS. Accelerated bioorthogonal conjugation: a practical method for the ligation of diverse functional molecules to a polyvalent virus scaffold. Bioconjug Chem 2005;16(6):1572–9.
[38] Chatterji A. Chemical conjugation of heterologous proteins on the surface of cowpea mosaic virus. Bioconjug Chem 2004;15(4):807–13.
[39] Kang S, Uchida M, O'Neil A, Li R, Prevelige PE, Douglas T. Implementation of p22 viral capsids as nanoplatforms. Biomacromolecules 2010;11(October 10):2804–9.
[40] Prevelige Jr PE, Thomas D, King J. Scaffolding protein regulates the polymerization of P22 coat subunits into icosahedral shells in vitro. J Mol Biol 1988;202(August (4)):743–57.
[41] Whitaker JR. An absolute method for protein determination based on difference in absorbance at 235 and 280 nm. Anal Biochem 1980;109(1):156.
[42] Hansen RE. Quantification of protein thiols and dithiols in the picomolar range using sodium borohydride and 4, 4′-dithiodipyridine. Anal Biochem 2007;363(1):77.
[43] Martos G. Egg white ovalbumin digestion mimicking physiological conditions. J Agric Food Chem 2010;58(9):5640–8.
[44] Moyron-Quiroz JE, Rangel-Moreno J, Hartson L, Kusser K, Tighe MP, Klonowski KD, et al. Persistence and responsiveness of immunologic memory in the absence of secondary lymphoid organs. Immunity 2006;25(October (4)):643–54.
[45] Matzinger P, Kamala T. Tissue-based class control: the other side of tolerance. Nat Rev Immunol 2011;11(March 3):221–30.
[46] Moyron-Quiroz JE, Rangel-Moreno J, Kusser K, Hartson L, Sprague F, Goodrich S, et al. Role of inducible bronchus associated lymphoid tissue (iBALT) in respiratory immunity. Nat Med 2004;10(September (9)):927–34.
[47] Matzinger P. Friendly and dangerous signals: is the tissue in control? Nat Immunol 2007;8(January (1)):11–3.
[48] Selin LK, Brehm MA, Kim SK, Chen HD. Heterologous immunity and the CD8 T cell network. Springer Semin Immunopathol 2002;24(2):149–68.
[49] Selin LK, Varga SM, Wong IC, Welsh RM. Protective heterologous antiviral immunity and enhanced immunopathogenesis mediated by memory T cell populations. J Exp Med 1998;188(November (9)):1705–15.
[50] Rangel-Moreno J, Carragher DM, Misra RS, Kusser K, Hartson L, Moquin A, et al. B cells promote resistance to heterosubtypic strains of influenza via multiple mechanisms. J Immunol 2008;180(January (1)):454–63.
[51] Wissinger E, Goulding J, Hussell T. Immune homeostasis in the respiratory tract and its impact on heterologous infection. Semin Immunol 2009;21(June (3)):147–55.
[52] Bachmann MF, Jennings GT. Vaccine delivery: a matter of size, geometry, kinetics and molecular patterns. Nat Rev Immunol 2010;10(November 11):787–96.
[53] Venter PA, Dirksen A, Thomas D, Manchester M, Dawson PE, Schneemann A. Multivalent display of proteins on viral nanoparticles using molecular recognition and chemical ligation strategies. Biomacromolecules 2011;12(June (6)):2293–301.
[54] Bachmann MF, Rohrer UH, Kundig TM, Burki K, Hengartner H, Zinkernagel RM. The influence of antigen organization on B cell responsiveness. Science 1993;262(November (5138)):1448–51.
[55] Chackerian B, Lenz P, Lowy DR, Schiller JT. Determinants of autoantibody induction by conjugated papillomavirus virus-like particles. J Immunol 2002;169(December (11)):6120–6.
[56] Pinschewer DD, Perez M, Jeetendra E, Bachi T, Horvath E, Hengartner H, et al. Kinetics of protective antibodies are determined by the viral surface antigen. J Clin Invest 2004;114(October (7)):988–93.
[57] Chackerian B, Durfee MR, Schiller JT. Virus-like display of a neo-self antigen reverses B cell anergy in a B cell receptor transgenic mouse model. J Immunol 2008;180(May (9)):5816–25.
[58] Bhagawati-Prasad VN, De Leenheer E, Keefe NP, Ryan LA, Carlring J, Heath AW. CD40mAb adjuvant induces a rapid antibody response that may be beneficial in post-exposure prophylaxis. J Immune Based Ther Vaccines 2010;8:1.